

Interlayer Coupling in Ferromagnetic Semiconductor Superlattices

T. Jungwirth^{1,2}, W.A. Atkinson¹, B.H. Lee¹, and A.H. MacDonald¹

¹*Department of Physics, Indiana University, Bloomington, Indiana 47405*

²*Institute of Physics ASCR, Cukrovarnická 10, 162 00 Praha 6, Czech Republic*

(February 1, 2008)

We develop a mean-field theory of carrier-induced ferromagnetism in diluted magnetic semiconductors. Our approach represents an improvement over standard RKKY model allowing spatial inhomogeneity of the system, free-carrier spin polarization, finite temperature, and free-carrier exchange and correlation to be accounted for self-consistently. As an example, we calculate the electronic structure of a $\text{Mn}_x\text{Ga}_{1-x}\text{As}/\text{GaAs}$ superlattice with alternating ferromagnetic and paramagnetic layers and demonstrate the possibility of semiconductor magnetoresistance systems with designed properties.

75.50.Pp, 75.70.Cn, 73.61.Ey, 75.70.Pa

Semiconductors and ferromagnetic materials play a largely complementary role in current information processing and storage technologies. The possibility of exploiting synergies between their properties has led to interest¹ in fabricating hybrid systems. Among these, the most widely studied are ones in which ferromagnetic metals are patterned on the surface of a semiconductor.² An attractive alternative has been presented by recent advances^{3–8} in the fabrication and control of diluted magnetic semiconductors which exhibit free-carrier induced ferromagnetism. In semiconductors, low intrinsic carrier densities allow electrical transport properties to be grossly altered by changing doping profiles or gate voltages. In ferromagnets, it is long range order which allows weak magnetic fields to reorient large moments and produce significant changes in transport and other properties. Systems with magnetically ordered free carriers in semiconductors open up a plethora of intriguing possibilities for engineered electronic properties. Since these will generally involve spatial patterning of dopant and magnetic ion densities, their description requires a theory of free-carrier induced ferromagnetism in semiconductors appropriate to inhomogeneous systems. In this Letter we present such a theory and apply it to the case of layered structures which mimic metallic giant-magnetoresistance multilayers.⁹ We conclude that strong magnetoresistance effects associated with half-metallic (fully polarized free-carrier band) states can occur in such systems.

The systems in which we are interested are described by Hamiltonians of the form

$$\mathcal{H} = \mathcal{H}_m + \mathcal{H}_f - J_{pd} \sum_{i,I} \vec{S}_I \cdot \vec{s}_i \delta(\vec{r}_i - \vec{R}_I). \quad (1)$$

Here \mathcal{H}_m is the Hamiltonian of localized spins \vec{S}_I , located at positions \vec{R}_I and interacting with an external magnetic field and, in general, also with each other. \mathcal{H}_f is the Hamiltonian of a semiconductor free-carrier system described using an envelope function¹⁰ language and including interactions of carriers with a random disorder

potential and with other carriers. We assume here that the semiconductor of interest has a single parabolic band; the formalism is readily generalized to multi-band situations which will often be of practical interest. The last term on the right-hand side of Eq. (1) represents the exchange interaction¹¹ between \vec{S}_I and free-carrier spins \vec{s}_i which is responsible for the novel physics. Our theory is simplified by the neglect¹² of dynamic correlations between a localized spin and both other localized spins and the free-carriers. We use a grand-canonical ensemble where the full system is in contact with a heat bath and the free carriers are in contact with a particle reservoir. Since we will ultimately use the local-spin-density approximation¹³ (LSDA) to account for correlations in the inhomogeneous free-carrier system, it is convenient to formulate our mean-field-theory in terms of the Gibbs thermodynamic variational principle which asserts that

$$\Omega \leq -k_B T \ln \left[\sum_{\alpha} \exp(-\langle \alpha | \mathcal{H} | \alpha \rangle / k_B T) \right]. \quad (2)$$

Here $|\alpha\rangle$ ranges over all possible direct products of localized spin moment m_I configurations and many-fermion free carrier states obtained by diagonalizing \mathcal{H} in subspaces with fixed localized spin configuration.

$$\langle \alpha | \mathcal{H} | \alpha \rangle = - \sum_I (g \mu_B B) m_I + E_{\kappa}[m_I], \quad (3)$$

where $E_{\kappa}[m_I]$ is a many-particle eigenvalue for free-carriers whose Hamiltonian includes the spin-dependent external potential term, $-\sum_i s_{z,i} [g^* \mu_B B + J_{pd} \sum_I m_I \delta(\vec{r}_i - \vec{R}_I)]$ with g and g^* denoting localized-spin and free-carrier g-factors respectively.

The sum over the many-fermion free-carrier states can be performed formally by appealing to spin-density-functional theory¹³ which states that the free-carrier grand potential can be expressed in terms of the ground state number and spin densities. Assuming that the total spin quantum number of each localized moment is S , it follows that

$$\Omega = \sum_I \Omega^{(0)}(b_I) + \Omega_f[n_\uparrow, n_\downarrow] - \frac{g^* \mu_B B}{2} \int d\vec{r} m(\vec{r}) \quad (4)$$

where $\Omega_f[n_\uparrow, n_\downarrow]$ is the internal free-carrier contribution, $b_I = [g\mu_B B + J_{pd}m(\vec{R}_I)/2]/k_B T$, and

$$\Omega^{(0)}(b_I) = -k_B T \ln \left[\sum_{i=-S}^S \exp(b_I i) \right] \quad (5)$$

is the thermodynamic potential of an isolated localized spin. In Eq. (4), $m(\vec{r}) = n_\uparrow(\vec{r}) - n_\downarrow(\vec{r})$ and the mean-field densities, $n_\uparrow(\vec{r})$ and $n_\downarrow(\vec{r})$, of the itinerant spins are to be adjusted so that the functional derivatives of Ω with respect to both $n_\uparrow(\vec{r})$ and $n_\downarrow(\vec{r})$ are identically equal to the chemical potential.

In spin-density functional theory practical self-consistent field calculations for inhomogeneous interacting fermions are made possible by the Kohn-Sham separation of Ω_f into single-particle, electrostatic and exchange-correlation pieces. The development here is standard apart from the introduction of an additional spin-dependent effective potential because of the dependence of b_I on $n_\uparrow(\vec{R}_I)$ and $n_\downarrow(\vec{R}_I)$. We find that the equilibrium free-carrier spin densities and the mean value of the localized spin quantum numbers on each site can be determined by solving the following equations self-consistently: i) a free-carrier single-particle Schrödinger equation with a spin-dependent potential,

$$\left[-\frac{\nabla^2}{2m^*} + V_\sigma(\vec{r}) \right] \psi_{k,\sigma}(\vec{r}) = \varepsilon_{k,\sigma} \psi_{k,\sigma}(\vec{r}), \quad (6)$$

where

$$V_\sigma(\vec{r}) = v_{es}(\vec{r}) + v_{xc,\sigma}(\vec{r}) - \frac{\sigma}{2} (g^* \mu_B B + h_{pd}(\vec{r}));$$

ii) the Poisson equation for the electrostatic potential

$$v_{es}(\vec{r}) = \frac{e^2}{\epsilon} \int d\vec{r}' \frac{n(\vec{r}')}{|\vec{r} - \vec{r}'|} + v_{ext}(\vec{r}), \quad (7)$$

where

$$n(\vec{r}) = n_\uparrow(\vec{r}) + n_\downarrow(\vec{r}), \quad n_\sigma(\vec{r}) = \sum_k f(\epsilon_{k,\sigma}) |\psi_{k,\sigma}(\vec{r})|^2,$$

$f(\epsilon_{k,\sigma})$ is the Fermi distribution function, and $v_{ext}(\vec{r})$ is the envelope function external potential¹⁰ including most importantly band edge and ionized impurity contributions; iii) the LSDA equation for the spin-dependent exchange-correlation potential

$$v_{xc,\sigma}(\vec{r}) = \frac{d[n\epsilon_{xc}(n_\uparrow, n_\downarrow)]}{dn_\sigma} \Big|_{n_\sigma = n_\sigma(\vec{r})}, \quad (8)$$

where $\epsilon_{xc}(n_\uparrow, n_\downarrow)$ is the exchange and correlation energy per particle of a spatially uniform free carrier system;¹⁵ iv) the mean-field equation for the exchange-coupling effective Zeeman field

$$h_{pd}(\vec{r}) = J_{pd} \sum_I \delta(\vec{r} - \vec{R}_I) \langle m_I \rangle, \quad (9)$$

where the mean-field localized-spin moment $\langle m_I \rangle = SB_S(b_I S)$ and $B_S(x)$ is the Brillouin function.¹⁴

For homogeneous systems with randomly distributed localized spins these equations can be solved analytically and represent an improvement over the mean-field theory RKKY interaction description of free-carrier induced ferromagnetism. Our approach allows finite temperature, free-carrier exchange and correlation, and free-carrier spin-polarization effects to be conveniently accounted for. The Curie-Weiss temperature, obtained from Eqs. (6)-(9), is given by

$$k_B T_c = \frac{cS(S+1)}{3} \frac{J_{pd}^2}{(g^* \mu_B)^2} \chi_f(n, T), \quad (10)$$

where c is the magnetic impurity density, and $\chi_f(n, T)$ is the temperature and density dependent free-carrier magnetic susceptibility. In Fig. 1 we have plotted the ferromagnetic transition temperature predicted by this expression for p -type $\text{Mn}_x\text{Ga}_{1-x}\text{As}$ with $S = 5/2$, $J_{pd} = 0.15 \text{ eV nm}^3$, $c = 10^{21} \text{ cm}^{-3}$ and hole mass $m^* = 0.5m_e$, as a function of free-carrier Fermi wavevector k_F .

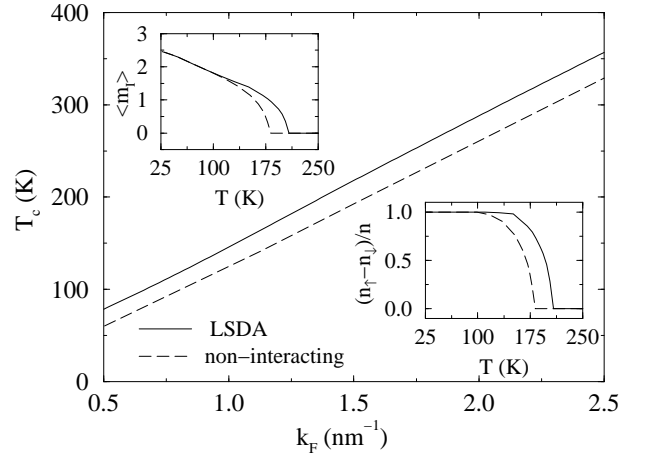


FIG. 1. Curie-Weiss temperature, as a function of free-carrier Fermi wavevector, calculated including (solid line) and neglecting (dashed line) the exchange-correlation potential. The localized spin moment (upper inset) and the free-carrier relative spin polarization (lower inset) are plotted as a function of temperature for $k_F = 1.4 \text{ nm}^{-1}$.

When exchange and correlation effects are neglected and $\chi_f(n, T)$ is replaced by its zero-temperature value, T_c is proportional to k_F and agrees with the RKKY theory expression.^{8,3,12} Free-carrier exchange and correlation enhances T_c by $\approx 30 \text{ K}$ in the range of free-carrier densities studied. The theory appears to be reasonably accurate when applied to the experimental systems we are interested in, those which have the largest critical temperatures³ ($T_c \approx 110 \text{ K}$), providing confidence in its application to inhomogeneous systems. It is not adequate

at small Mn fraction ($x < 0.02$) where ferromagnetism is not observed, presumably because the free-carrier density is below its Mott limit. Experimentally, T_c also decreases for $x > 0.07$, possibly because of spin-fluctuation effects neglected in the mean-field theory¹². The insets in Fig. 1 show that in the density-range of interest, the magnetization of the localized spins saturates more slowly than that of the free carriers as the temperature falls below the critical temperature.

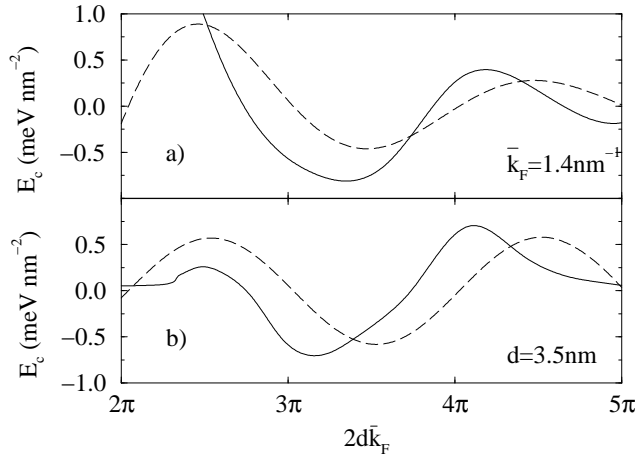


FIG. 2. Interlayer exchange coupling (solid lines) as a function of the Mn-undoped GaAs spacer thickness (a) and as a function of the average density of free-carriers (b). The dashed lines is the RKKY interaction coupling energy calculated with all magnetic impurities confined to planes separated by the superlattice period. Results are plotted as a function of dimensionless parameter $2d\bar{k}_F$.

Once the band edge and ionized and magnetic impurity profiles have been specified, Eqs. (6)-(9) can be used to solve for the system's equilibrium properties. As an illustration of our approach, we consider a $\text{Mn}_x\text{Ga}_{1-x}\text{As}/\text{GaAs}$ superlattice with magnetic impurities in alternate layers. We look for two different self-consistent solutions of Eqs. (6)-(9), a ferromagnetic (F) one with parallel ordered moments in all Mn-doped regions, and a solution with an antiferromagnetic (AF) alignment of adjacent magnetic layers. The interlayer exchange coupling E_c , is defined as the difference in energy between AF and F-states per area per $\text{Mn}_x\text{Ga}_{1-x}\text{As}$ layer and is expected¹⁶ to oscillate with GaAs spacer width. In Fig. 2 we present numerical results for E_c as a function of a dimensionless parameter $2d\bar{k}_F$ where \bar{k}_F is the Fermi wavevector corresponding to the average 3D density of free carriers in the superlattice with a period d . The system we consider has 2 nm thick $\text{Mn}_x\text{Ga}_{1-x}\text{As}$ layers with $c = 10^{21} \text{ cm}^{-3}$ and homogeneously distributed ionized impurities that neutralize free-carrier charge. Oscillations in the self-consistent (solid lines) E_c , are qualitatively consistent with simple RKKY model estimates;¹⁶ differences exist primarily because of the proximity induced spin-polarization in the nominally paramagnetic

GaAs layers mentioned below. The amplitude of oscillations in E_c is $\sim 10\times$ smaller than in metallic systems¹⁷ measured in absolute units and $\sim 10\times$ larger if energy is measured relative to the Fermi energy of free carriers. In order to achieve substantial exchange coupling in experimental systems it will be important to limit disorder scattering in the GaAs layers.

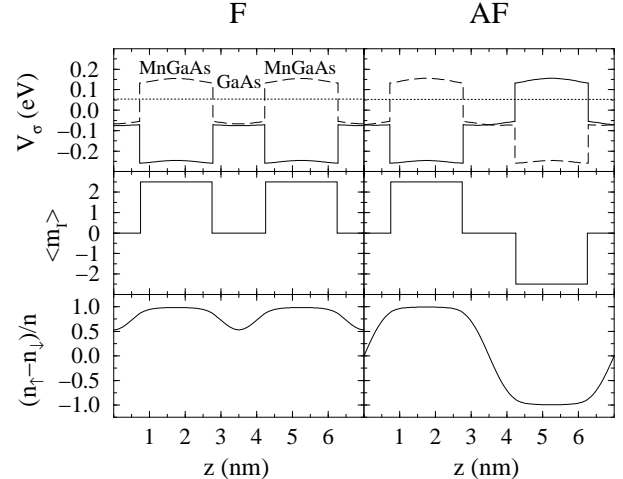


FIG. 3. Self-consistent results plotted within the unit cell of the $\text{Mn}_x\text{Ga}_{1-x}\text{As}/\text{GaAs}$ superlattice. From top to bottom: i) effective potentials from Eq. 6 for up (solid lines) and down (dashed lines) spin free-carriers (the dotted line here indicates the chemical potential); ii) mean-field localized spin moment; iii) free-carrier relative spin-polarization.

Our mean-field calculation also yields information on the localized and free-carrier spin magnetization densities and on the spin-split bands of the free-carrier system. This information provides a starting point for building a theory of electronic transport. Numerical results for the above $\text{Mn}_x\text{Ga}_{1-x}\text{As}$ superlattice with $d = 3.5 \text{ nm}$ and $\bar{k}_F = 1.4 \text{ nm}^{-1}$ (corresponding to average density 10^{20} cm^{-3}) are summarized in Figs. 3 and 4. In the top panels of Fig. 3, the chemical potential and the effective potentials for spin-up and spin-down free carriers (see Eq. (6)) are plotted as a function of z over a AF configuration unit cell. All energies here and below are measured from the spatial average of the electrostatic potential $v_{es}(z)$. The potentials V_σ have similar shapes in F and AF cases, except for the reversed order for up and down spins in the right Mn-doped layer. Note that in this example, confinement of carriers in the magnetic layers is due entirely to the exchange potential produced by magnetic order. The localized (middle panels) and itinerant (lower panels) spin systems reach 100 % polarization in the Mn-doped layers at the temperature ($T = 0.1T_c$) and carrier density for which these calculations were performed. The itinerant system spin-polarization is large in the layers free of magnetic impurities, especially so in the F-state case.

Fig. 4 shows occupied minibands in the superlattice Brillouin zone. In the F-state spin-up and spin-down

minibands are split by about 0.25 eV. There is no spin-splitting in the AF-state since the effective potentials V_{\uparrow} and V_{\downarrow} differ by a rigid shift in the \hat{z} direction. The miniband dispersion is much weaker in the AF case because the barriers separating two adjacent minima in the effective potential are twice as thick and high as in the F case. Since the conductance is approximately proportional to the square of the largest miniband width in either coherent or incoherent transport limits, the minibands can be used to estimate the size of the current-perpendicular-to-plane (CPP) magnetoresistance effect. For the case illustrated, the AF state CPP conductance will be three orders of magnitude smaller than the F state CPP conductance. The large difference is expected since the bulk $\text{Mn}_x\text{Ga}_{1-x}\text{As}$ bands are half-metallic for these parameters. In general we predict strong CPP magnetoresistance in $\text{Mn}_x\text{Ga}_{1-x}\text{As}/\text{GaAs}$ multilayer systems if the AF state can be realized.

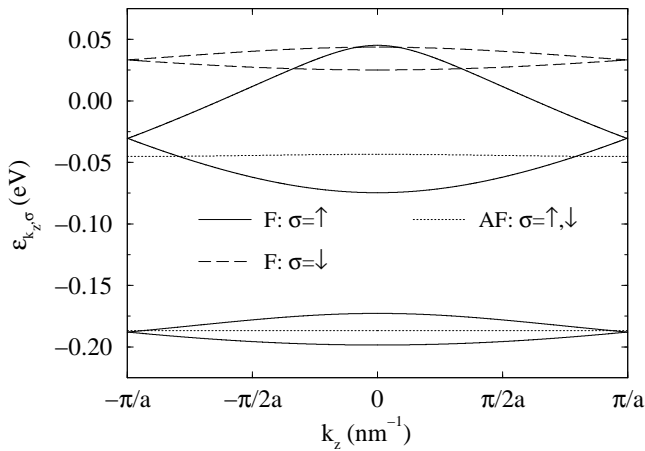


FIG. 4. Partially occupied energy minibands in F-state for spin-up (solid line) and spin-down (dashed line). In the AF-state both spins (dotted line) have the same minibands. The chemical potential is 0.053 eV and $a=7$ nm is the unit cell length.

The $\text{GaAs}/\text{Mn}_x\text{Ga}_{1-x}\text{As}$ superlattice is but one example of a semiconductor nanostructure to which our mean field theory can be applied. Tremendous flexibility is possible even within systems containing only GaAs based materials. These can act like a normal (N) conductor, like an itinerant ferromagnet (F) when a fraction of the Ga atoms is replaced by Mn, and like an insulator (I) when a large enough fraction of Ga in the crystal is replaced by Al. In GaAs-based N/F/I heterostructures all components are lattice matched and have relatively simple band structures. Geometries of interest include F-N junctions, N-F-N spin-filters, F-N-F spin-valves, and F-I-F magnetic tunnel junctions. Since the materials are semiconductors rather than metals, external bias voltages can have a strong influence on both charge and magnetization density profiles. Self-consistency is hence essential in modeling these systems.

The authors acknowledge helpful interactions with D.D. Awschalom, J.K. Furdyna. and E. Miranda. This work was supported by the National Science Foundation under grants DMR-9623511, DMR-9714055 and INT-9602140, by the Ministry of Education of the Czech Republic under grant ME-104 and by the Grant Agency of the Czech Republic under grant 202/98/0085.

- ¹ See for example G. Prinz, *Physics Today* **48**, 58 (1995).
- ² P. Ye *et al.* *Phys. Rev. Lett.* **74**, 3013 (1995); *ibid* *Semicond. Sci. Technol.* **11**, 1613 (1996); H.A. Carmona, A.K. Geim, A. Norgaret, P.C. Main, T.J. Foster, and A. Henini, *Phys. Rev. Lett.* **74**, 3009 (1995).
- ³ H. Ohno, *Science* **281**, 951 (1998); H. Matsukura *et al.*, *Phys. Rev. B* **57**, R2037 (1998); H. Ohno *et al.*, *Appl. Phys. Lett.* **69**, 363 (1996); H. Ohno *et al.*, *Phys. Rev. Lett.* **68**, 2664 (1992).
- ⁴ S. Koshihara *et al.*, *Phys. Rev. Lett.* **78**, 4617 (1997).
- ⁵ A. Van Esch *et al.*, *Phys. Rev. B* **56**, 13103 (1997).
- ⁶ T. Story *et al.*, *Phys. Rev. Lett.* **56**, 777 (1986).
- ⁷ A. Haury *et al.*, *Phys. Rev. Lett.* **79**, 511 (1997); I.P. Smorchkova *et al.* *Phys. Rev. Lett.* **78**, 3571 (1997).
- ⁸ T. Dietl, A. Haury, and Y. Merle d'Aubigné, *Phys. Rev. B* **55**, R3347 (1997).
- ⁹ For a review see B. Heinrich and J.A.C. Bland, *Ultrathin Magnetic Structures*, Vol. 2 (Springer, Berlin, 1994).
- ¹⁰ G. Bastard, *Wave Mechanics Applied to Semiconductor Heterostructures* (Les Éditions de Physique, Paris, 1990).
- ¹¹ J.K. Furdyna, *J. Appl. Phys.* **64**, R29 (1988); *Semimagnetic Semiconductors and Diluted Magnetic Semiconductors*, edited by M. Averous and M. Balkanski (Plenum, New York, 1991); T. Dietl in *Handbook on Semiconductors*, Chap. 17 (Elsevier, Amsterdam, 1994).
- ¹² Homogeneous ferromagnetic semiconductors are closely related to the low-carrier-concentration limit of dense Kondo systems, which is well-described by mean-field theory; Manfred Sigrist, Kazuo Ueda, and Hirokazu Tsunetsugu, *Phys. Rev. B* **46**, 175 (1992).
- ¹³ R.M. Dreizler and E.K.U. Gross, *Density Functional Theory: An Approach to the Quantum Many-Body Problem* (Springer, Berlin, 1990); N. Argaman and G. Makov, preprint [cond-mat/9806013] (1998).
- ¹⁴ A. Aharoni, *Introduction to the theory of ferromagnetism* (Clarendon Press, Oxford, 1996).
- ¹⁵ S.H. Vosko *et al.*, *Can. J. Phys.* **58**, 1200 (1980).
- ¹⁶ A. Yfet, *Phys. Rev. B* **36**, 3948 (1987).
- ¹⁷ Discrepancies exist between experimental and ideal theoretical values of E_c in metallic systems, partly because of interface roughness effects (J. Kudrnovsky *et al.*, *Phys. Rev. B* **53**, 5125 (1996)). This comparison with metallic systems is based on E_c values for Fe/Au/Fe triplelayers where good agreement is found between theory and experiment: J. Ugrundis *et al.*, *Phys. Rev. Lett.* **79**, 2734 (1997).